International Journal of Innovative
Computing, Information and Control
Volume 8, Number 12, December 2012

 ISSN 1349-4198
pp. 8473–8485

FAULT DIAGNOSIS FOR A CLASS OF NONLINEAR DIGITAL SENSORS BASED ON OUTPUT TRACKING

Fang Deng[1,2], Jie Chen[1,2] and Lishuang Xu[1,2]

[1]School of Automation
Beijing Institute of Technology
[2]Key Laboratory of Complex System Intelligent Control and Decision Ministry of Education
5 South Zhongguancun Street, Haidian District, Beijing 100081, P. R. China
dengfang@bit.edu.cn

Received October 2011; revised March 2012

Abstract. *This paper focuses on fault diagnosis for a class of digital sensors. The first derivative and second derivative of these sensors' output signal under normal conditions will not involve a great jump due to physical limitations. It is similar to maneuvering targets which do not exhibit particularly jump in velocity and acceleration. So, a real-time random sensor fault diagnosis is transformed into a maneuvering target tracking problem. And a fault diagnosis method independent on system models is proposed. An improved unscented Kalman filter (UKF) is employed to track the output and estimate the value of various states. A mean-adaptive acceleration (MAA) model is established to find the faults of digital sensors online. According to the analysis of the failure characteristics in different sampling conditions, a method is proposed to isolate the faults. Theoretical analysis and experimental results show that the method can diagnose and isolate digital sensor fault accurately in real applications.*

Keywords: Fault diagnosis, Sensors, Improved UKF, MAA

1. **Introduction.** Numerous sensors are applied in almost all industrial mechatronic system, and any fault of the sensors could be extremely deteriorate system performance, or even cause systems to break down. Fault diagnosis of sensors helps to ensure the normal operation of the system.

Sensor fault diagnosis methods can be grouped into two categories: model-based approaches and knowledge-based approaches [1, 2]. Model-based approaches make use of quantitative analytical models of a physical system. Knowledge-based approaches do not need full analytical modeling and allow one to use qualitative models based on the available information and knowledge of a physical system [3]. Kalman filter and its improved forms as a kind of typical model-based approaches were adopted in [4, 5, 6, 7, 8] to estimate model parameters which reflect the states of sensors. These methods have a good real-time performance. However, the plant model that the Kalman filter and most information fusion approaches rely on is difficult to obtain in actual applications. For systems which are hard to model, the characteristic data which are analyzed and extracted from mass data are used for fault diagnosis. Consequently, the model-based methods are not applicable. In order to relax the restrictions on system models, the knowledge-based approaches use qualitative models based on available information and knowledge of the system to detect and isolate faults [9, 10, 11, 12]. Wavelet transformation was also utilized by many scholars to analyze the output signal of sensors [13, 14, 15]. Nevertheless, these methods can only detect the failure but fail to isolate the effect of sensor faults. Besides, real-time sensor fault diagnosis is one of the difficult issues for Knowledge-based

approaches, especially when the sensor's output is a random signal and the true value of its current point cannot be obtained.

A fault diagnosis method for a class of digital sensors independent on system models and true values is proposed in this paper. We found that general sensors' output data under normal conditions, the first derivative and second derivative of the signal are smooth without jump, as maneuvering targets like aircrafts do not appear particularly jump in velocity and acceleration due to physical conditions. The real-time random sensor fault diagnosis is transformed into a maneuvering target tracking problem. Output signals of digital sensors are tracked and the values of various states are estimated by filters. A mean-adaptive acceleration (MAA) model is established to find the faults of digital sensors online. Some inherent characteristics of this kind of digital sensors are utilized to isolate the different kinds of failures.

This paper is organized as follows. Section 2 presents the digital sensor definitions and main fault features. Section 3 presents the real-time fault detection method based on improved UKF. Section 4 gives the fault location method. Experimental results are demonstrated in Section 5, and concluding remarks are given in Section 6.

2. Problem Statement and Preliminaries.

This section gives the description of a class of digital sensor and the failure characteristics of the digital sensors in uniform sampling and random sampling. The characteristics of a class of digital sensor are described from Equation (1) to (3).

The sensor's output $y(k)$ is a linear combination of n sub-functions,

$$y(k) = \sum_{i=1}^{n} g_i(x_j) \quad j = 1, 2, \cdots, \kappa \tag{1}$$

where k is the sampling instant, sub-function $g_i(x_j)$ is a periodic function which consists of finite states ($\leq \kappa$). The occurring probability of each state is equal in any sampling period with cycle T_i (frequency f_i).

The sub-functions satisfy the following relation matrix:

$$\frac{T_i}{T_j} = \frac{f_j}{f_i} = \mathbf{W}_{ij} = \begin{bmatrix} 1 & c_{12} & \cdots & c_{1n} \\ c_{21} & 1 & \cdots & c_{2n} \\ \vdots & \vdots & \ddots & \vdots \\ c_{n1} & c_{n2} & \cdots & 1 \end{bmatrix} \tag{2}$$

where $\mathbf{W}_{ij}$ is the relation matrix for sub-functions. In this matrix, the following relationship is holds:

$$c_{ij} = \frac{1}{c_{ji}} = \kappa^{i-j} \quad i = 1 \cdots n, \;\; j = 1 \cdots n \tag{3}$$

Remark 2.1. *The output of this kind of digital sensors, such as the parallel port angle sensors, which convert analog data to digital data through A/D converters, can be described by Equation (1) to (3), as every bit of the digital data has different weights. And for binary(κ) sensors, each bit of the digital data has two (κ ary) states. Therefore, the specific expression of $g_i(x_j)$ depends on the band and weight. For example, the $g_i(x_j)$ can be expressed as follows in binary case:*

$$g_i(x_i) = 2^{i-1} x_i \quad x_i \in \{0, 1\} \tag{4}$$

Binary digital angle sensor is a very commonly used sensor. A whole circle is represented as a binary weighted sum. For example, an n-bit absolute optical encoder divides

a 360-degree circle into 2^n. The weight of each bit is 2^{i-1}. Its measured output value can be expressed with the following statement.

$$y(k) = \sum_{i=1}^{n} 2^{i-1} x_i(k), \quad x_i(k) \in \{0, 1\} \tag{5}$$

2.1. **The failure characteristics under uniform sampling.** In uniform sampling conditions, the true value of sampling points can be directly calculated from time or reference value provided by other sensors. Set the true value to be $y^*(k)$, and the relationship between the measured value and the reference value is given as follows:

$$y(k) = y^*(k) + f_k \mathbf{\Omega} \tag{6}$$

where f_k is the failure function at point k, $\mathbf{\Omega}$ is the fault matrix with elements value 1(0) in failure(normal) case.

Definition 2.1. *In uniform sampling condition, the main failure mode of sensor is defined as follows:*

(1) *Complete failure:*

$$\mathbf{\Omega}^T y^*(k) + f_k = \delta \tag{7}$$

where δ is a constant, and for any sampling point, the output is a constant.

(2) *Deviation:*

$$f_k = f_{k-1} = \delta \tag{8}$$

The output value is biased with a constant.

(3) *Drift:*

$$f_k = f_{k-1} - \delta, \quad f_0 = 0 \tag{9}$$

The measured values are corrupted by both constant and trend terms.

(4) *Accuracy decline:*

$$E(f_k) = 0, \quad E\left(f_k^2\right) = \sigma_f^2 = \delta^2 \tag{10}$$

The output value is normal in a single detection, but the failure function is subjected to a certain probability distribution.

2.2. **The failure characteristics under random sampling.** There is no reference value for fault feature extraction in random sampling conditions. Therefore, fault characteristics should be associated with sampling conditions.

Definition 2.2. *The main failure mode of the sensors in random sampling is defined as follows:*

(1) *Complete failure: For any sub-wire i, there exist*

$$g_i(x_j) = \delta, \quad \forall i \tag{11}$$

where δ is a constant. For any sampling point, the output is a constant.

(2) *Partial failure: For some sub-wire i, there exist*

$$g_i(x_j) = \delta \tag{12}$$

3. **Real-Time Fault Detection Based on Output Tracking.** In this section, we use the improved UKF to detect the real-time fault.

The fault diagnosis method based on Kalman filters needs to obtain the system model and the sensor model. However, in practice, it is difficult to build the model of the sensor and get the true value of sensor without using other instruments. In this case, the sensor's output is assumed to be a target and an improved UKF is utilized as an estimator to track the sensor's output. Consequently, the sensor fault detection is transferred into a target tracking problem. The improved UKF is employed to track the output and estimate the value of various states. A MAA model is established to find the faults of digital sensors online.

Suppose that the sensor output is a function of time t, $x(t)$, the velocity of output is $\dot{x}(t)$, and the acceleration is $\ddot{x}(t)$. The acceleration of the sensor output cannot be accurately obtained in real applications, and the mean of acceleration is assumed not to be zero. A 'current' model (MAA) [22] is adopted to represent the sensor's output. The model of the MAA is presented as follows:

$$\begin{aligned} X_{k+1} = & \begin{bmatrix} 1 & T & \left(-1+\alpha T+e^{-\alpha T}\right)/\alpha^2 \\ 0 & 1 & \left(1-e^{-\alpha T}\right)/\alpha \\ 0 & 0 & e^{-\alpha T} \end{bmatrix} X_k \\ & + \begin{bmatrix} (T^2/2)-\left(-1+\alpha T+e^{-\alpha T}\right)/\alpha^2 \\ T-\left(1-e^{-\alpha T}\right)/\alpha \\ 1-e^{-\alpha T} \end{bmatrix} \bar{a}_k + w_k \end{aligned} \tag{13}$$

where k indicates the kth step of state estimation filter; T is the sampling period, $a = \ddot{x}$ is acceleration; w_k is the state noise at step k; $\alpha = 1/\tau$, and τ is the system maneuver time. $\bar{a}_k$ is the mean of current acceleration and $\bar{a}_k$ can be expressed as [23]:

$$\begin{aligned} \bar{a}_{k+1} &= E[a_{k+1} \left| z^k \right.] \\ &= e^{-\alpha T} E[a_k \left| z^k \right.] + \left(1-e^{-\alpha T}\right) \bar{a}_k \\ &= e^{-\alpha T} \hat{a}_k + \left(1-e^{-\alpha T}\right) \bar{a}_k \end{aligned} \tag{14}$$

As the maneuver time constant τ increases (i.e., αT decreases), the Singer model reduces to the Constant Acceleration (CA) model.

The MAA model has a good tracking performance. It can track and estimate the output value. In the case of failures, the sensor's output will be abnormal and the value of position estimation in tracking model will jump, thus the mean of position estimation will have offset. The velocity and acceleration values are hopping or outside the normal range. This method can be adopted as a real-time fault detection method for sensor failures.

The traditional maneuvering target tracking methods, such as the EKF (extended Kalman filter), UKF [16, 17] and PF [18, 19] (particle filter), can be utilized to track the sensors' outputs. When there is a fault in the digital sensor, its output exists jump signal. Thus the traditional EKF that is used to track the output is often divergent or unstable. Particle filtering is a sequential Monte Carlo simulation based on nonlinear filtering algorithms. The main problem with PF is the degradation of particles [18]. After several iterations, only a small number of particles have greater weight and the weight of other particles is approximately zero. Meanwhile, particle filters have to face a serious computational burden when they are applied to estimate the parameters and states in output tracking.

UKF is a nonlinear filter with high precision, strong stability and small computational burden. Because of its robustness and stability [20, 21], it is satisfactory for UKF to solve strongly nonlinear problems.

For tracking and estimating the output sinal of digital sensors, the improved UKF algorithm is utilized to improve the tracking ability of common UKF.

(1) Compute the Sigma points and weights [24, 25]

The n-dimensional random variable x_k with mean $\hat{x}_k$ and covariance P_k is approximated by $2n+1$ weighted samples or *sigma points* selected by the algorithm

$$\chi_k = \left[\begin{array}{ccc} \hat{x}_k & \hat{x}_k + \left(\sqrt{(n+\eta)\,P_k}\right)_i & \hat{x}_k - \left(\sqrt{(n+\eta)\,P_k}\right)_i \end{array} \right] \tag{15}$$

$$W_0^{(m)} = \eta/(n+\eta) \tag{16}$$

$$W_0^{(c)} = \eta/(n+\eta) + (1-\alpha^2+\beta) \tag{17}$$

$$W_i^{(m)} = W_i^{(c)} = 1/(2n+2\eta), \quad i = 1, \cdots, 2n \tag{18}$$

$$\eta = \alpha^2(n+\zeta) - n \tag{19}$$

where $\left(\sqrt{P_k}\right)_i$ is the ith row or column of the matrix square root of P_k, and W_i is the weight associated with the ith point, and η is a scaling parameter. The parameter α determines the spread of the sigma points around $\hat{x}_k$ and is usually set to be a small positive value (e.g., 0.001). ζ is a secondary scaling parameter which is usually set to be 0, and β is used to incorporate prior knowledge of the distribution of x_k (for Gaussian distributions, $\beta = 2$ is optimal).

(2) State prediction

Sigma-point will be substituted into the nonlinear state equation and observation equation, the transformation Sigma-points are evaluated for each of the $0-2n$ points by

$$\chi_{k+1|k} = f(\chi_k) \tag{20}$$

The mean of transformed set of sigma points $\hat{x}_{k+1|k}$ is computed by

$$\hat{x}_{k+1|k} = \sum_{i=0}^{2n} W_i^{(m)} \chi_{i,k+1|k} \tag{21}$$

The predicted observation is computed by

$$\gamma_{k+1/k} = h\left(\chi_{k+1/k}\right) \tag{22}$$

$$\hat{y}_{k+1/k} = \sum_{i=0}^{2n} W_i^{(m)} \gamma_{i,k+1|k} \tag{23}$$

and the predicted covariance is computed by

$$P_{k+1|k} = \lambda_{k+1} \sum_{i=0}^{2n} W_i^{(c)} \left[\chi_{i,k+1|k} - \hat{x}_{k+1|k}\right] \left[\chi_{i,k+1|k} - \hat{x}_{k+1|k}\right]^T + Q \tag{24}$$

where $\chi_{i,k+1|k}$ and $\gamma_{i,k+1|k}$ are the ith row of $\chi_{k+1|k}$ and $\gamma_{k+1|k}$ respectively.

(3) Measurement update

Compute the covariance and the cross correlation matrix by

$$P_{x_{k+1}y_{k+1}} = \lambda_{k+1} \sum_{i=0}^{2n} W_i^{(c)} \left[\chi_{i,k+1|k} - \hat{x}_{k+1|k}\right] \left[\gamma_{i,k+1|k} - \hat{y}_{k+1/k}\right]^T \tag{25}$$

$$P_{y_{k+1}y_{k+1}} = \lambda_{k+1} \sum_{i=0}^{2n} W_i^{(c)} \left[\gamma_{i,k+1|k} - \hat{y}_{k+1/k}\right] \left[\gamma_{i,k+1|k} - \hat{y}_{k+1/k}\right]^T + R_{k+1} \tag{26}$$

$$K_{k+1} = P_{x_{k+1}y_{k+1}} P^{-1}_{y_{k+1}y_{k+1}} \tag{27}$$

Then update the mean and covariance

$$P_{k+1} = P_{k+1|k} - K_{k+1} P_{y_{k+1}y_{k+1}} K^T_{k+1} \tag{28}$$

$$\hat{x}_{k+1} = \hat{x}_{k+1|k} + K_{k+1}\left(y_{k+1} - \hat{y}_{k+1/k}\right) \tag{29}$$

where $\lambda_{k+1} \geq 1$ is a fading factor.

The parameter λ_{k+1} is computed as (30)-(36):

$$\lambda_{i,k+1} = \psi_i c_{k+1}, \quad i = 1, 2, \cdots, n \tag{30}$$

where ψ and ζ are pre-defined constants; c_{k+1} is a factor to be determined, which is computed as follows:

$$\lambda_{k+1} = \begin{cases} \psi c_{k+1} & \zeta \leq c_{k+1} \\ c_{k+1} & 1 \leq c_{k+1} < \zeta \\ 1 & c_{k+1} \leq 1 \end{cases} \tag{31}$$

$$c_{k+1} = \frac{tr\left(\mathbf{N}_{k+1}\right)}{tr\left(\mathrm{M}_{k+1}\right)} \tag{32}$$

$$\mathrm{N}_{k+1} = tr\left[\mathbf{V}_{0,k+1} - \mathbf{R}_{k+1}\right] \tag{33}$$

$$\mathbf{M}_{k+1} = \sum_{i=0}^{2n} W_i \left[\Delta_{i,k+1|k} - \hat{y}_{k+1/k}\right]\left[\Delta_{i,k+1|k} - \hat{y}_{k+1/k}\right]^T \tag{34}$$

$$\mathbf{V}_{0,k+1} = \begin{cases} \mathbf{\Delta}_1 \mathbf{\Delta}_1^T, & k = 0 \\ \frac{\rho \mathbf{V}_{0,k} + \mathbf{\Delta}_{k+1}\mathbf{\Delta}^T_{k+1}}{1+\rho}, & k \geq 1 \end{cases} \tag{35}$$

$$\mathbf{\Delta}_{k+1} = \mathbf{Y}_{k+1} - \hat{\mathbf{Y}}_{k+1/k} \tag{36}$$

When the failures are detected by the improved UKF, we should locate and isolate the fault, thus the specific fault location methods based on the characteristics of the data will be given in the following section.

4. Fault Location Method.

This paper uses the statistical and relative change characteristics to detect and isolate faults. The steps of fault isolation are presented as follows.

4.1. The statistical fault characteristics of random sampling data.

Theorem 4.1. *For the sensor described in Equation (1) to (3) in a certain period of time, when the sample number far exceeds the number of its states, and the sampling value of the sub-wire contains various states of the sub-wire, the average of each wire data is close to*

$$E(g_i(x_j)) = \frac{\sum_{j=1}^{\kappa} x_j}{\kappa} \tag{37}$$

where κ is the maximum number of every possible state for the sensor's each wire. Meanwhile, the greater the number of samples is, more the average of each wire data is more close to left of (37).

Proof: From Equation (1) to (3), $g_i(x_j)$ is a periodic function and its state number is not more than κ. The probability of each state appears to be the same in a full cycle. Denote the probability of each state that appears by $P_j(x_j)$, the sample number by K and the number of each sampled state by k_j. The following statements hold.

$$\sum_{j=1}^{\kappa} k_j = K \tag{38}$$

$$\sum_{j=1}^{\kappa} P_j(x_j) = 1 \tag{39}$$

The sum of all states is

$$\sum_{j=1}^{\kappa} k_j x_j = K\left(\sum_{j=1}^{\kappa} P_j(x_j)x_j\right) \tag{40}$$

The mean of every wire is

$$E(g_i(x_j)) = \frac{\sum\limits_{j=1}^{\kappa} k_j x_j}{K} \tag{41}$$

If the number of sampling points is sufficient, the probability to cover each state is closer:

$$\begin{aligned} E\left(g_i(x_j)\right) = \frac{\sum\limits_{j=1}^{\kappa} k_j x_j}{K} &\approx \frac{K\left(\sum\limits_{j=1}^{\kappa} P_j(x_j)x_j\right)}{K} \\ &= \sum_{j=1}^{\kappa} P_j(x_j)x_j = \sum_{j=1}^{\kappa} \frac{1}{\kappa} x_j = \frac{\sum\limits_{j=1}^{\kappa} x_j}{\kappa} \end{aligned} \tag{42}$$

when $K \to \infty$, the approximately equal sign of (42) can become an equal sign.

Remark 4.1. *According to Theorem 4.1, for a binary sensor, it is known that $\kappa = 2$, namely, the mean of each wire data is close to 0.5.*

The fault location operation based on Theorem 4.1 can be given as follows:

Step 1: Sampling. It is better that the sampling number is as many as possible and the sampling rate is as uniform as possible. The large the sampling number is, the more precise the diagnostic result is.

Step 2: Compute the mean of each wire.

Step 3: Failure location. If the mean of each wire is far away from (41), the sampling values tend to some constants, the sampling period of the wire is the short one and the sampling state is to cover all of the state changes, it is a wire failure. If all of the state changes are not covered, the number of sampling need to be increased.

Step 4: Precision diagnosis. The closer to 0.5 the mean is, the better its quality and the lower the probability of failure is. The higher-weight bits have greater impact on sensor output precision.

4.2. **The relative change characteristics of random sampling data.** The statistical method based on Theorem 4.1 locates faults by the mean of digital sensor all wire status. The method requires that the number of samples is large enough, only when the number of samples is large enough and the sampling is uniform, its conclusion would be more accurate. The method's real-time performance is limited as relies on a large amount of calculation. To solve these problems, we give the following definition:

Definition 4.1. *State change number: The number of the digital sensor's bit change.*

Remark 4.2. *For the sensor described in Equation (1) to (3), the state change number is κ in one period. For example, for a binary sensor, assume that there are five sampling points. The lowest bit data is 01010, $0 \to 1 \to 0 \to 1 \to 0$, so that the state changes four times in a cycle; the second lowest bit data is 00110, $0 \to 0 \to 1 \to 1 \to 0$, the state change number is 2.*

Based on Definition 4.1, a new theorem is proposed as follows:

Theorem 4.2. *For the sensor which satisfies Equation (1) to (3), assume that the sampling number is K and the sampling data range is γ $(0 \leq \gamma)$, then the state change number is proportional to the frequency of each wire, and the state change number between different sensor wires satisfy the following relation:*

$$\frac{m_j}{m_i} \approx \mathbf{W}_{ij} = \begin{bmatrix} 1 & c_{21} & \cdots & c_{n1} \\ c_{12} & 1 & \cdots & c_{n2} \\ \vdots & \vdots & \ddots & \vdots \\ c_{1n} & c_{2n} & \cdots & 1 \end{bmatrix} \tag{43}$$

$$c_{ij} = \frac{1}{c_{ji}} = \kappa^{i-j} \quad i, j = 1 \cdots \alpha \tag{44}$$

$$c_{ij} = c_{ji} = 0 \quad i > \alpha \ \text{ or } \ j > \alpha \tag{45}$$

where α is the highest bit's value that is not zero and in the normal data range. The range satisfies the following relation

$$\kappa^{\alpha-1} \leq \gamma \leq \kappa^{\alpha} \tag{46}$$

Meanwhile, the larger the number of samples included in the state is, the closer to $\mathbf{W}_{ij}$ the ratio is. When the sample data is insufficient, the state change number ratio of higher bits is closer to (43) than lower bits.

Proof: From Equation (1) to (3), $g_i(x_j)$ is a period function, and satisfies (2), hence

$$\frac{T_i}{T_j} = \frac{f_j}{f_i} = \mathbf{W}_{ij} = \begin{bmatrix} 1 & c_{12} & \cdots & c_{1n} \\ c_{21} & 1 & \cdots & c_{2n} \\ \vdots & \vdots & \ddots & \vdots \\ c_{n1} & c_{n2} & \cdots & 1 \end{bmatrix}$$

When the sampling range satisfies the following condition

$$\kappa^{n-1} \leq \gamma \leq \kappa^{n} \tag{47}$$

the state change number of each bit satisfies following relation

$$\frac{m_j}{m_i} = \frac{T_i}{T_j} = \frac{f_j}{f_i} \tag{48}$$

When the sampling range cannot cover all the change

$$\alpha < n \tag{49}$$

the state change number of the wire which satisfies $j > \alpha$ is 0, namely

$$m_j = 0, \quad j > \alpha \tag{50}$$

where α is the highest bit value that the sampling data is not zero.

The relation of low bit state change number is as follows:

$$\frac{m_j}{m_i} \approx \frac{T_i}{T_j} = \frac{f_j}{f_i} \tag{51}$$

As the sampling is random, lower bits change fast. If the sampling interval is too large, it will miss some relevant information, so the left and right side of (51) approximately equal. The larger the sample number and state is, the closer the two sides of (51).

From (48) to (51), we can draw the conclusions in Theorem 4.2.

According to Theorem 4.2, for binary sensors, we know $\kappa = 2$, and the sampling scope is $2^{n-1} \leq \gamma$. The state change number of the sensor ith bit satisfies the following formula:

$$m_i = 2^{n-i+1} - 1 \tag{52}$$

Theorem 4.2 can be utilized to locate the failure without specific sample values and other sensors to provide any the calibration. The state change numbers are recorded and employed to locate the failure. To record the change number is easier than to measure sensors' frequency, period or to calculate the average. It is suitable for real-time fault location and application in embedded systems.

The fault location step based on Theorem 4.2 is as follows:

Step 1: Sampling.

Get as many samples as possible. The larger the sampling number is, the more precise the diagnostic result is. Even if the sampling number is not enough, the conclusion of Theorem 4.2 is also holds.

Step 2: Record the state change number of each bit m_i, $i = 1, \cdots, n$.

Step 3: Find the bit α with largest weight. The α is decided by sampling range γ, $\kappa^{\alpha-1} \leq \gamma \leq \kappa^{\alpha}$.

Step 4: Normalization processing

$$\bar{m}_i = \frac{m_i}{\kappa^{\alpha-i}}, \quad i = 1, \cdots, n \tag{53}$$

From (47) and (53), when $i > \alpha$:

$$\bar{m}_i = m_i = 0, \quad i = \alpha + 1, \cdots, n \tag{54}$$

From (53) and (54), the criterion to locate the fault is

$$\bar{m}_i = \begin{cases} 1 & i = 1, \cdots, \alpha \\ 0 & i = \alpha + 1, \cdots, n \end{cases} \tag{55}$$

Step 5: Failure location

From (55), when $\bar{m}_i$ satisfies (55), the wire is normal. When the sampling is not enough, the low bit is short of data, so its normalized value is less than 1. If the value is far less than 1, it is a fault wire.

For a better description of the method of this paper, the algorithm flow chart is shown in Figure 1.

5. **Experiment Results.** In the experiment, we take a 15-bit absolute optical encoder as an example shown in Figure 2. Absolute optical encoder is a very commonly used sensor. A whole circle is represented as a binary weighted sum. For example, a 15-bit absolute optical encoder divides a 360-degree circle into 2^{15}. The weight of each bit is 2^{i-1}. Its measured output value can be expressed with the following statement.

$$y(k) = \sum_{i=1}^{15} 2^{i-1} x_i(k), \quad x_i(k) \in \{0, 1\} \tag{56}$$

A test bench [26] is utilized in the experiment. The sampling time and rotation step of the test bench can be changed according to different experiments. The figure of the test bench is shown is Figure 2.

We utilize the test bench to simulate real work conditions of the encoder and record the encoder's outputs. We simulated parallel port optical encoder common types of failure, disconnection, short circuit and grounding.

First, a normal recorder is rotated manually and the data are recorded by test bench. The normal signal is the first subgraph of Figure 3. The estimation results of states

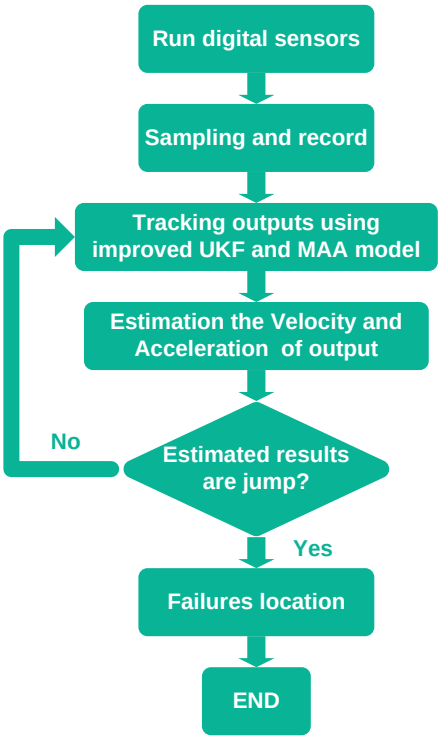

FIGURE 1. The flow chart of fault diagnosis

FIGURE 2. The test bench

including position estimation, velocity estimation and acceleration estimation are shown from the second subgraph to fourth subgraph of Figure 3. We can see from Figure 3 that states of the recorder output signal are smooth, so the recorder is normal.

Then, the results of the 5th experiment with faults and failures are shown in Figure 4. As shown in Figure 4, there are some representative jump points which are marked out in figure. These points are adopted to indicate that the fault happen and we use fault location method described in Section 4 to locate faults.

There are five experiments for testing the algorithm of fault diagnosis and the test results are shown in Table 1.

Remark 5.1. *In Table 1, A indicates that the fault mode of disconnection, B indicates that the fault mode of short circuit and C indicates that the fault mode of grounding. The first column is the serial number of the experiment. The fault-bit number and failure modes*

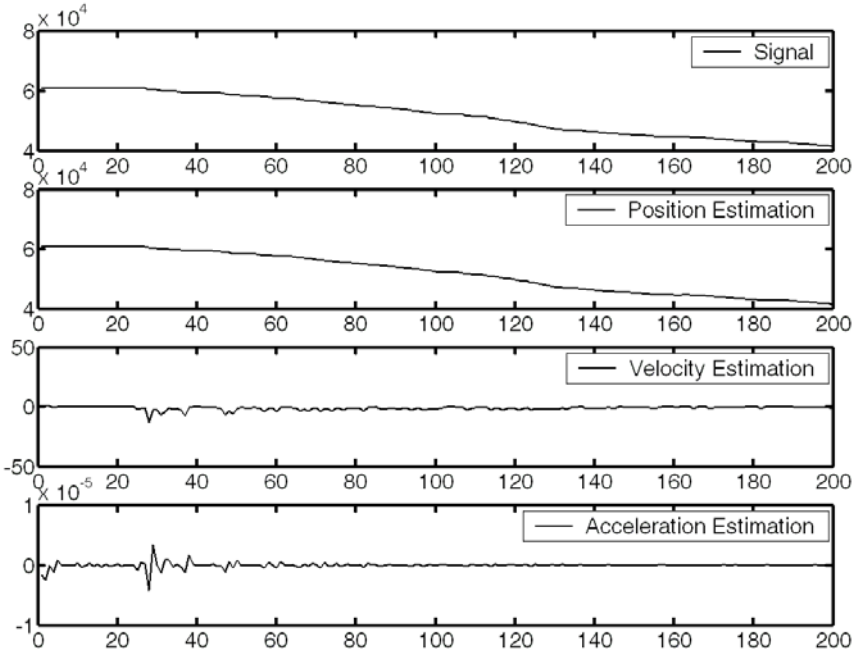

FIGURE 3. Tracking results of manual random sampling under normal conditions

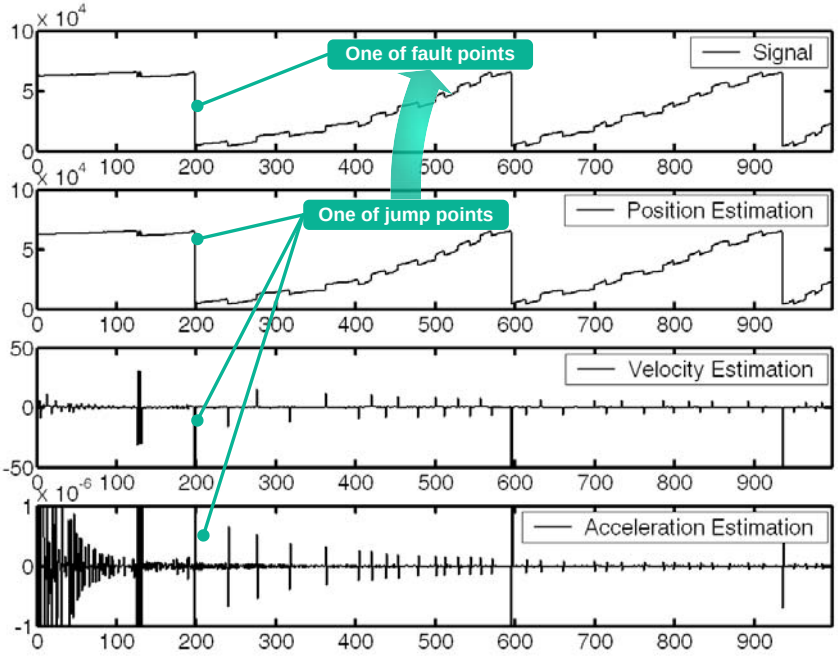

FIGURE 4. Tracking results of manual random sampling under fault conditions

of the absolute optical encoder are located in the second and third columns respectively. The fourth is a list of the number of sampling points. The fifth column is sample range. The sixth column is mean of fault bits according to the Theorem 4.1. The seventh column is the mean of all normal data. The eighth column is the state change number according

TABLE 1. The results of fault diagnosis

No.	Real Fault		Fault Diagnosis						
	Fault bit	Fault mode	Sampling number	Sampling range	Mean of fault bit	Mean of normal bit	State change number of fault bit	Fault bit	Fault mode
1	6	A	200	63°	1	0.5542	6: 0	6	A
2	14	A	200	240°	1	0.4773	14: 0	14	A
3	12, 13	B	200	360°	0.695	0.5100	12, 13: 7	12, 13	B
4	2 7 12	A A A	997	800°	1 1 1	0.5166	2: 0 7: 0 12: 0	2 7 12	A A A
5	5 8 4, 10	A C B	499	600°	1 0 0.7512	0.5301	5: 0 8: 0 4, 10: 158	5 8 4, 10	A C B

to the Theorem 4.2. The last column fault diagnosis result including the fault location and the fault mode.

From Table 1, the proposed method can accurately diagnose short-circuit, disconnection and grounding fault of photoelectric encoder. Even multiple simultaneous faults can be accurately diagnosed.

6. **Conclusion.** The improved UKF is employed to track the output and estimate the value of various states, and a Mean-Adaptive Acceleration (MAA) model is established to find the faults of digital sensors online which are widely used in digital control and calibration systems. Through analyzing failure characteristics, we propose different methods to isolate different kinds of failures. Theoretical analysis and experimental results show that our method can diagnose and isolate digital sensor fault accurately, and it is a practical fault diagnosis and isolation method.

Acknowledgment. This work has been supported in part by Projects of Major International (Regional) Joint Research Program NSFC under Grants No. 61120106010 and National Science Fund for Distinguished Young Scholars of China under Grants No. 60925011.

REFERENCES

[1] P. Li and V. Kadirkamanathan, Particle filtering based likelihood ratio approach to fault diagnosis in nonlinear stochastic systems, *IEEE Transactions on Systems, Man and Cybernetics, Part C: Applications and Reviews*, vol.31, no.3, pp.337-343, 2001.

[2] T. Wei, Y. Huang and C. Chen, Adaptive sensor fault detection and identification using particle filter algorithms, *IEEE Transactions on Systems, Man and Cybernetics, Part C: Applications and Reviews*, vol.39, no.2, pp.201-213, 2009.

[3] C. Qi, P. K. Varshney and C. M. Belcastro, Fault detection in dynamic systems via decision fusion, *IEEE Transactions on Aerospace and Electronic Systems*, vol.44, no.1, pp.227-242, 2008.

[4] W. Xue, Y.-Q. Guo and X.-D. Zhang, Application of a bank of Kalman filters and a robust Kalman filter for aircraft engine sensor/actuator fault diagnosis, *International Journal of Innovative Computing, Information and Control*, vol.4, no.12, pp.3161-3168, 2008.

[5] W. Li, L. S. Sirish and D. Xiao, Kalman filters in non-uniformly sampled multirate systems: For FDI and beyond, *Automatica*, vol.44, no.1, pp.199-208, 2008.

[6] D. Zhou, A new approach to sensor fault detection and diagnostics of nonlinear systems, *Acta Automatica Sinica*, no.3, pp.362-365, 1995.
[7] X. Xu, X. Wang and H. Zhang, Sensors fault-diagnosis based on accommodation Kalman filter, *Chinese Journal of Scientific Instrument*, no.S1, pp.79-80, 2005.
[8] H. Chingiz and C. Fikret, Sensor/actuator fault diagnosis based on statistical analysis of innovation sequence and robust Kalman filtering, *Aerospace Science and Technology*, vol.4, no.6, pp.415-422, 2000.
[9] J. M. Abdel and L. Reza, A hybrid intelligent system for fault detection and sensor fusion, *Applied Soft Computing*, vol.9, no.1, pp.415-422, 2009.
[10] D. L. Yu, J. B. Gomm and D. Williams, Sensor fault diagnosis in a chemical process via RBF neural networks, *Control Engineering Practice*, vol.7, no.1, pp.49-55, 1999.
[11] K. Salahshoor, M. Mosallaei and M. Bayat, Centralized and decentralized process and sensor fault monitoring using data fusion based on adaptive extended Kalman filter algorithm, *Measurement*, vol.41, no.10, pp.1059-1076, 2008.
[12] F. Afef, H. Xu and N. C. Fahmida, Neural networks based system identification techniques for model based fault detection of nonlinear systems, *International Journal of Innovative Computing, Information and Control*, vol.3, no.5, pp.1073-1085, 2007.
[13] M. Oussama, L. Dimitri, K. Mohamad, H. Ghaleb and C. Houcine, Fault detection algorithm using DCS method combined with filters bank derived from the wavelet transform, *International Journal of Innovative Computing, Information and Control*, vol.5, no.5, pp.1313-1327, 2009.
[14] X. Xu, F. Xiao and S. Wang, Enhanced chiller sensor fault detection, diagnosis and estimation using wavelet analysis and principal component analysis methods, *Applied Thermal Engineering*, vol.28, no.2-3, pp.226-237, 2008.
[15] J. Qi and J. Han, Application of wavelets transform to fault detection in rotorcraft UAV sensor failure, *Journal of Bionic Engineering*, vol.4, no.4, pp.265-270, 2007.
[16] S. Sadhu, S. Mondal, M. Srinivasan and T. K. Ghoshal, Sigma point Kalman filter for bearing only tracking, *Signal Processing Special Section: Multimodal Human-Computer Interfaces*, vol.86, no.12, pp.3769-3777, 2006.
[17] P. Li, T. Zhang and B. Ma, Unscented Kalman filter for visual curve tracking, *Image and Vision Computing Statistical Methods in Video Processing*, vol.22, no.2, pp.157-164, 2004.
[18] A. M. Sanjeev, M. Simon, G. Neil and C. Tim, A tutorial on particle filters for online nonlinear/non-Gaussian Bayesian tracking, *IEEE Transactions on Signal Processing*, vol.50, no.2, pp.174-188, 2002.
[19] N. J. Gordon, D. J. Salmond and A. F. Smith, Novel approach to nonlinear/non-Gaussian Bayesian state estimation, *Radar and Signal Processing, IEE Proceedings F*, vol.140, no.2, pp.107-113, 1993.
[20] N. Cui, L. Hong and J. R. Layne, A comparison of nonlinear filtering approaches with an application to ground target tracking, *Signal Processing*, vol.85, no.8, pp.1469-1492, 2005.
[21] B. G. Saulson and K. C. Chang, Nonlinear estimation comparison for ballistic missile tracking, *Optical Engineering*, vol.43, no.6, pp.1424-1438, 2004.
[22] H. Zhou and K. S. P. Kumar, A 'current' statistical model and adaptive algorithm for estimating maneuvering targets, *Journal of Guidance, Control, and Dynamics*, vol.7, no.5, pp.596-602, 1984.
[23] L. X. Rong and V. P. Jilkov, Survey of maneuvering target tracking. Part I. Dynamic models, *IEEE Transactions on Aerospace and Electronic Systems*, vol.39, no.4, pp.1333-1364, 2003.
[24] S. Julier, J. Uhlmann and H. F. Durrant-Whyte, A new method for the nonlinear transformation of means and covariances in filters and estimators, *IEEE Transactions on Automatic Control*, vol.45, no.3, pp.477-482, 2000.
[25] S. J. Julier, The scaled unscented transformation, *Proc. of American Control Conference*, pp.4555-4559, 2002.
[26] F. Deng, J. Chen, W. Chen and C. Chi, High precision test method and apparatus for photoelectric encoder, *Transaction of Beijing Institute of Technology*, vol.27, no.11, pp.977-980, 2007.